J. Appl. Comput. Mech., 5(5) (2019) 840-848
DOI: 10.22055/JACM.2019.28313.1476

ISSN: 2383-4536
jacm.scu.ac.ir

M&MoCS

Shahid Chamran
University of Ahvaz

Journal of
Applied and Computational Mechanics

Research Paper

Irreversibility Analysis of MHD Buoyancy-Driven Variable Viscosity Liquid Film along an Inclined Heated Plate Convective Cooling

A.S. Eegunjobi[1], O.D. Makinde[2]

[1] Mathematics Department, Namibia University of Science and Technology
Windhoek, 9000, Namibia, Email: samdet1@yahoo.com

[2] Faculty of Military Science, Stellenbosch University
Private Bag X2, Saldanha 7395, South Africa, Email: makinded@gmail.com

Received January 21 2019; Revised February 11 2019; Accepted for publication February 13 2019.
Corresponding author: A.S. Eegunjobi samdet1@yahoo.com

Abstract. Analysis of intrinsic irreversibility and heat transfer in a buoyancy-driven changeable viscosity liquid along an incline heated wall with convective cooling taking into consideration the heated isothermal and isoflux wall is investigated. By Newton's law of cooling, we assumed the free surface exchange heat with environment and fluid viscosity is exponentially dependent on temperature. Appropriate governing model equations for momentum and energy balance with volumetric entropy generation expression are obtained and then transformed using dimensionless variables to form set of nonlinear boundary valued problem. Using shooting method with Runge-Kutta-Fehlberg integration scheme, the model is numerically tackled. Pertinent results for the fluid velocity, temperature, skin friction, Nusselt number, entropy generation rate and Bejan number are obtained and discussed.

Keywords: Inclined plane; MHD liquid film; Isothermal wall; Isoflux wall; Convective cooling; Entropy generation

1. Introduction

Flowing down in an inclined wall refer to liquid film, it plays a vital role in the development of well-planned means for interfacial heat and mass transfer in many engineering applications. The flow of liquid films in an inclined wall has several applications such as in wetting phase systems, polymeric systems, hydrodynamics and surface coating, detergency, flotation, condensation.

Due to its applications, several works have been carried out on thin liquid films [1-3]. Makinde [4] investigated the thermal stability of boundary layer flow of a temperature-dependent viscosity liquid film with adiabatic free surface along an inclined heated plate using special type Hermite-Pade approximation techniques. The study revealed accurate steady-state thermal criticalities conditions. Sadiq and Usha [5] assumed constant temperature gradient and studied linear instability of a thin layer of viscoelastic fluid flowing down a non-uniformly heated inclined plane. Analytical solution of a laminar falling variable viscosity liquid film along an inclined heated plate was considered by Makinde [6].

Investigation of flow with temperature dependent liquid viscosity is of great importance in hemodynamic, lubrication, hot shaping (glasses), viscometry and various engineering applications. Several researches' work in various dimensions have been carried out on temperature dependent viscosity. Sekhar and Jayalatha [7] used normal modes and Galerkin method to investigate a linear stability analysis of convection in viscoelastic liquids with temperature-dependent viscosity. Nonino *et al.* [8] carried out a parametric analysis on the effects of temperature dependent viscosity in simultaneously developing laminar flow of a liquid in straight ducts of arbitrary but constant cross-section. Hooman and Gurgenci [9] studied temperature-

Published online: May 18 2019

dependent viscosity variation effect on Benard convection, of a gas or a liquid, in an enclosure filled with a porous medium based on the general model of momentum transfer in a porous medium. Kabova *et al.* [10] performed numerical and theoretical investigations of the heat transfer and hydrodynamics in a liquid film flowing along an inclined substrate under the action of gravity with a local heat source. Entropy generation is the parameter used to establish energy efficiency limit in engineering devices. Entropy production analysis of fluid flow in various geometries have been researched by many authors. Eegunjobi and Makinde [11] investigated numerically the entropy generation rate in a transient variable viscosity Couette flow between two concentric pipes. Ganesh *et al.* [12] investigated the Newtonian fluid flow problem with buoyancy and thermal radiation in non-linear form by considering the entropy generation. Afridi *et al.* [21] presented the non-similar solution of MHD mixed convection flow using the Sparrow-Quack-Boerner local non-similarity method. Khan *et al*. [22] investigated three-dimensional axisymmetric steady flow of micropolar fluid over a rotating disk in a slip-flow regime.

Magnetohydrodynamics (MHD) is of great interest in industrial applications. It is characterized by the observation of the magnetic field which improves fluid viscosity and hence rises the flow resistance. Many works considered the effect of magnetic field on flow structures in various dimensions. Eegunjobi and Makinde [13] considered the combined effects of magnetic field, buoyancy force, velocity slip, suction/injection, porous medium permeability, thermal radiation absorption, viscous and Joule heating on mixed convective flow of an electrical conducting Casson fluid in a vertical channel. Sourtiji *et al*. [14] carried out numerical analysis of magnetic field effect on free convection heat transfer in a horizontal cylindrical-triangular annulus filled with copper-water nanofluid. The effect of magnetic field on mathematical model of blood flow through an overlapping stenosed artery with core region was considered by Parma *et al.* [15].

In this present study, we examine the intrinsic irreversibility and heat transfer characteristics of a buoyancy-driven variable viscosity liquid along an incline isothermal and isoflux heated surface with convective cooling. The model problem is numerically investigated. The effects of various embedded parameters on the velocity profile, temperature profile, skin friction, Nusselt number, entropy generation rate and the Bejan number are presented graphically and discussed.

2. Mathematical Formulation

We consider MHD buoyancy-driven flow of a Newtonian incompressible and electrically conducting liquid film along an inclined isothermal or isoflux wall as shown in figure 1. It is assumed that the fluid viscosity is exponentially dependent on temperature. The slight variation in the fluid density due to temperature difference is assumed to follow Bousinessq approximation while the rest of the fluid properties remain constants.

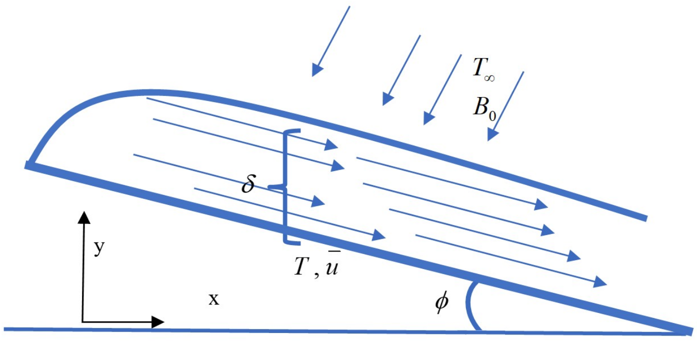

Fig. 1. Problem geometry

Under these assumptions, the continuity, momentum, energy and volumetric entropy generation equations take the form [16-19]

$$\frac{\partial \bar{u}}{\partial \bar{x}} = 0 \tag{1}$$

$$\frac{d}{d\bar{y}}\left(\bar{\mu}\frac{d\bar{u}}{d\bar{y}}\right) - \sigma B_0^2 \bar{u} + \rho g \beta \left(T - T_\infty\right)\sin\left(\phi\right) = 0 \tag{2}$$

$$\rho c_p \bar{u}\frac{\partial T}{\partial \bar{x}} = k\frac{\partial^2 T}{\partial \bar{y}^2} + \bar{\mu}\left(\frac{d\bar{u}}{d\bar{y}}\right)^2 + \sigma B_0^2 \bar{u}^2 \tag{3}$$

$$E_g = \frac{k}{\left(T_w - T_\infty\right)^2}\left[\left(\frac{\partial T}{\partial \bar{x}}\right)^2 + \left(\frac{\partial T}{\partial \bar{y}}\right)^2\right] + \frac{\bar{\mu}}{\left(T_w - T_\infty\right)}\left[\frac{\partial \bar{u}}{\partial \bar{y}}\right]^2 + \frac{\sigma B_0^2 \bar{u}^2}{\left(T_w - T_\infty\right)} \tag{4}$$

The boundary conditions for us to explore both isothermal and isoflux heated in an incline wall surface are written as

$$\bar{u}=0, \quad ak\frac{\partial T}{\partial \bar{y}}=\frac{kb}{\delta}\left(T-T_{\infty}\right)-\frac{k}{\delta}\left(T_w-T_{\infty}\right) \quad \text{at } \bar{y}=0 \tag{5}$$

Isoflux heating occurs where $a=1,\ b=0$ and isothermal heating takes place where $a=0,\ b=1$. The convective heating trade-off with the surrounding at the free surface is written as

$$\frac{d\bar{u}}{d\bar{y}}=0,\ -k\frac{\partial T}{\partial \bar{y}}=h\left(T-T_{\infty}\right) \quad \text{at } \bar{y}=\delta \tag{6}$$

where $\bar{u}$ represents axial velocity, δ is the thickness of liquid film, ϕ is the angle of inclination, B_0 is the magnetic field acting perpendicular to the liquid film flow, T is the absolute temperature, T_{∞} is the surrounding temperature, T_w is the wall temperature, h represents heat transfer coefficient, k is thermal conductivity, ρ is the density of the fluid, $\bar{x},\bar{y}$ are horizontal and vertical distance respectively, g is acceleration due to gravity, β is volumetric thermal expansion coefficient, c_P is specific heat at constant pressure while a and b are inclined wall heating parameters. We can express the viscosity temperature dependency as:

$$\bar{\mu}(T)=\mu_0 e^{-\gamma(T-T_{\infty})} \tag{7}$$

where μ_0 is viscosity of the fluid at surrounding temperature and γ ascertains the strength of impact between temperature and viscosity. In addition, the fluid axial temperature gradient is assumed to be constant. Introducing the following dimensionless variables gives:

$$\left.\begin{aligned}
&x=\frac{\bar{x}}{\delta},\quad \eta=\frac{\bar{y}}{\delta},\quad \theta=\frac{T-T_{\infty}}{T_w-T_{\infty}},\ w=\frac{\bar{u}\delta}{\nu_0},\ \nu_0=\frac{\mu_0}{\rho},\ \frac{d\theta}{dx}=A,\mathrm{Pr}=\frac{\mu_0 c_P}{k}\\
&m=\gamma\left(T_w-T_{\infty}\right),\ M=\frac{\sigma B_0^2\delta^2}{\mu_0},\ Ra=\frac{g\beta\delta^3\left(T_w-T_{\infty}\right)}{\nu_0^2},\ Bi=\frac{h\delta}{k},Ec=\frac{\nu_0^2}{\delta^2 c_P\left(T_w-T_{\infty}\right)}
\end{aligned}\right\} \tag{8}$$

Incorporating equation (8) into equations (2-7), we obtain,

$$\frac{d^2w(\eta)}{d\eta^2}-m\frac{d\theta(\eta)}{d\eta}\frac{dw(\eta)}{d\eta}-Mw(\eta)e^{m\theta(\eta)}+Ra\theta(\eta)e^{m\theta(\eta)}\sin\left(\phi\right)=0 \tag{9}$$

$$\frac{d^2\theta(\eta)}{d\eta^2}-\mathrm{Pr}w(\eta)A+\mathrm{Pr}Ec\left(\frac{dw}{d\eta}\right)^2 e^{-m\theta(\eta)}+MEc\,\mathrm{Pr}\left(w(\eta)\right)^2=0 \tag{10}$$

$$Ns=A^2+\left[\frac{d\theta(\eta)}{d\eta}\right]^2+\mathrm{Pr}Ec\left[\frac{dw(\eta)}{d\eta}\right]^2 e^{-m\theta(\eta)}+M\ \mathrm{Pr}Ecw(\eta)^2 \tag{11}$$

with

$$\left.\begin{aligned}
&w=0,\ a\frac{d\theta(\eta)}{d\eta}=b\theta(\eta)-1 \qquad at \qquad \eta=0\\
&\frac{dw}{d\eta}=0,\ \frac{d\theta(\eta)}{d\eta}=-Bi\,\theta(\eta) \qquad at \qquad \eta=1
\end{aligned}\right\} \tag{12}$$

where Bi denotes Biot number, Pr is Prandtl number, Ec is the Eckert number, M is the magnetic field parameter, Br (=$EcPr$) is the Brinkmann number and A is constant. Other parameters of concentration are Nusselt number (Nu), skin friction coefficients (Cf), the Bejan number (Be), irreversibility due to heat transfer (N_1), Rayleigh number (Ra) and entropy generation due to viscous dissipation (N_2) defined as

$$Nu=\frac{\delta q_w}{k\left(T_w-T_{\infty}\right)}=-\left.\frac{d\theta(\eta)}{d\eta}\right|_{\eta=0},\quad Cf=\frac{\delta^2\tau_w}{\rho\nu_0^2}=e^{-m\theta(\eta)}\left.\frac{dw(\eta)}{d\eta}\right|_{\eta=0},\ Be=\frac{N_1}{Ns}=\frac{1}{1+\lambda} \tag{13}$$

where

$$\left.\begin{array}{l} q_w = -k \left.\dfrac{dT}{d\bar{y}}\right|_{\bar{y}=0}, \tau_w = \bar{\mu}\left.\dfrac{d\bar{u}}{d\bar{y}}\right|_{\bar{y}=0}, \quad N_1 = A^2 + \left[\dfrac{d\theta(\eta)}{d\eta}\right]^2, \quad \lambda = \dfrac{N_2}{N_1}, \\ N_2 = \Pr Ec\left[\dfrac{dw(\eta)}{d\eta}\right]^2 e^{-m\theta(\eta)} + M \Pr Ec w(\eta)^2. \end{array}\right\} \tag{14}$$

3. Numerical Procedure

Equations (9)-(10) together with boundary conditions (12) are the dimensionless models representing the boundary value problems (BVP). These equations are converted into set of nonlinear first order ordinary differential equations together with unspecified initial conditions to be determined by shooting procedures. Assume

$$w = z_1, w' = z_2, \theta = z_3, \theta' = z_4 \tag{15}$$

Then $z_1' = z_2$, $z_3' = z_4$. Therefore, the dimensionless governing equations becomes

$$\left.\begin{array}{l} z_2' = mz_4 z_2 + Mz_1 e^{mz_3} - Raz_3 e^{mz_3}\sin(\phi), \\ z_4' = \Pr z_1 A - \Pr Ec z_2^2 e^{-mz_3} - MEc \Pr z_1^2 \end{array}\right\} \tag{16}$$

with initial conditions as

$$z_1(0)=0, z_2(0)=c_1, z_3(0)=0, z_4(0)=c_2 \tag{17}$$

The unspecified initial conditions c_1 and c_2 are guessed first and then determined by using Newton Raphson techniques according to prescribed boundary conditions for each set of parameter values. We solve numerically the outcome of initial value problem by adopting Runge-Kutta-Fehlberg integration scheme [20]. In our computation, we assume $A = 1$.

3. Results and Discussion

The effect of increasing angle of inclination (ϕ), magnetic field parameter (M), Rayleigh number (Ra), Eckert number (Ec) and Biot number (Bi) on fluid velocity profiles for both isothermal and isoflux are presented in figures 2-5. As can be seen in figures 2 and 3, the increased angle of inclination and magnetic field parameter for both cases decrease the fluid velocity profiles. Besides, the maximum fluid velocity is attained at the free surface with lowest angle of inclination. The decrease in both cases at the free surface is attributed to high fluid viscous forces on the fluid velocity equation and proportion of magnetic induction to viscous forces. Meanwhile in these figures, the increase in Rayleigh number accelerates the fluid velocity at the free surface for both isothermal and isoflux walls. The increase in Rayleigh number caused the buoyancy forces to increase. This therefore leads to decrease in thermal boundary layer thickness at the free surface and in turn increase the fluid velocity Figure 4 and 5 present the effects of Ec and Bi on the velocity profile. It is shown that increase in Ec has no effect on the flow velocity in isothermal wall but increases the fluid velocity in isoflux wall at free surface. Moreover, as Biot number increases, the fluid velocity profiles for both isothermal and isoflux decreases at the free surface walls.

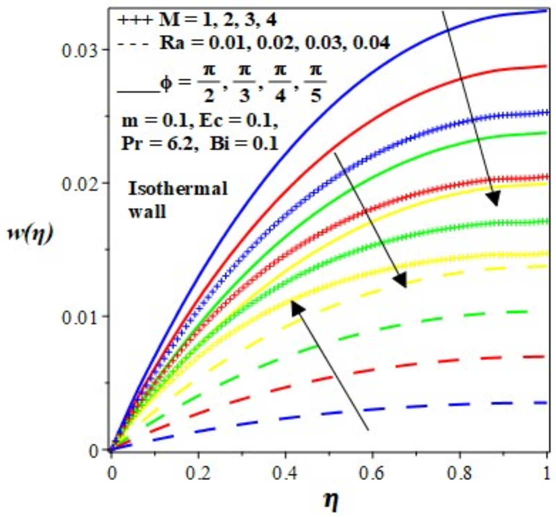

Fig. 2. Velocity profile with increasing ϕ, M and Ra

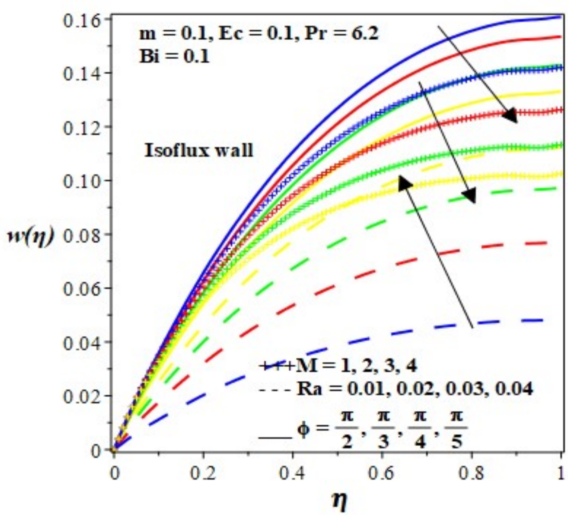

Fig. 3. Velocity profile with increasing ϕ, M and Ra

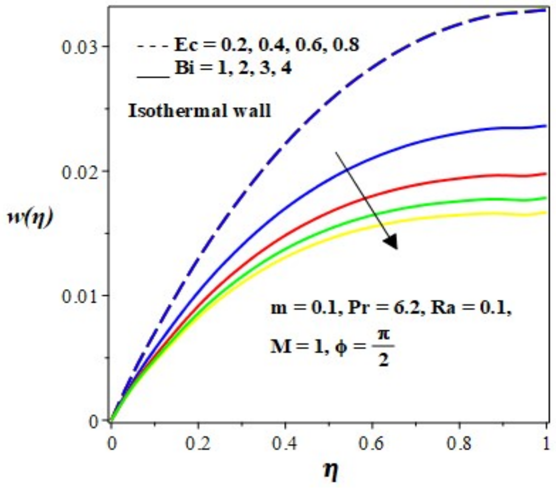

Fig. 4. Velocity profile with increasing *Bi* and *Ec* numbers

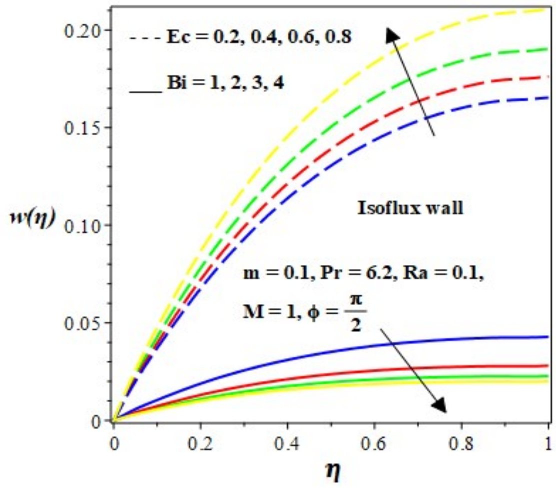

Fig. 5. Velocity profile with increasing *Bi* and *Ec* numbers

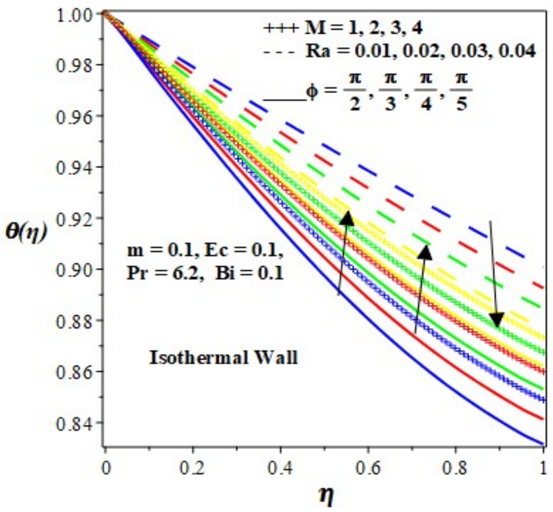

Fig. 6. Temperature profile with increasing ϕ , *M* and *Ra*

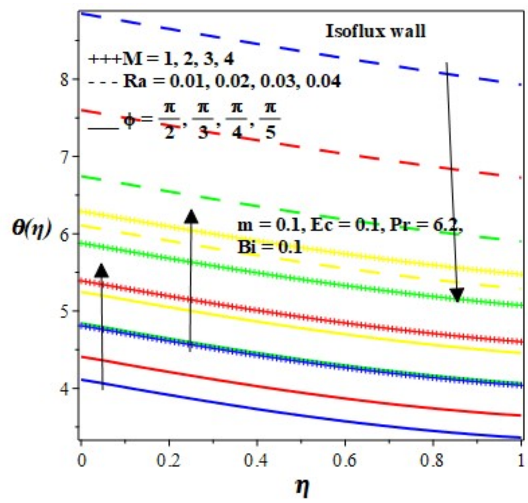

Fig. 7. Temperature profile with increasing ϕ , *M* and *Ra*

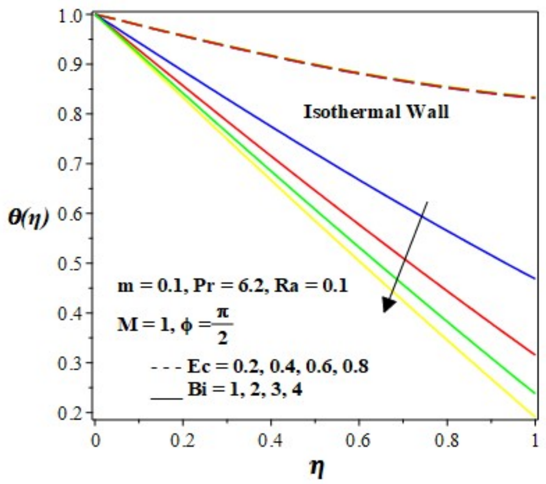

Fig. 8. Temperature profile with increasing *Bi* and *Ec* numbers

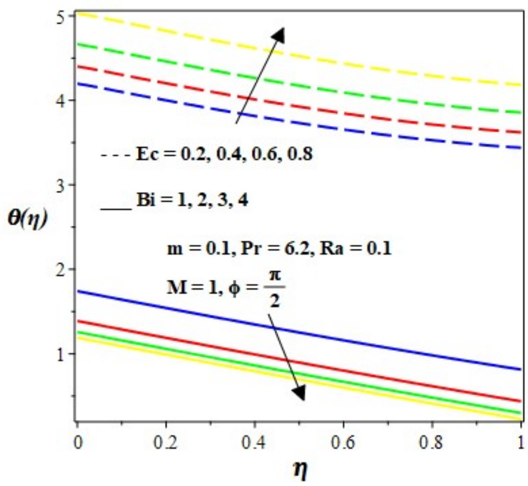

Fig. 9. Temperature profile with increasing *Bi* and *Ec* numbers

Figures 6-9 depict the consequences of angle of inclination, magnetic field parameter (*M*), Rayleigh number (*Ra*), Eckert number (*Ec*) and Biot number (*Bi*) on fluid temperature profiles. In figure 6, the fluid temperature united at the wall surface and gradually increased towards the free surface as ϕ and *M* are increasing but decrease at free surface as Ra is increasing. The situation at the wall surface corroborates the boundary condition. At the wall surface, the intermolecular forces get stronger and thereby increase the viscosity and as it proceeds, the intermolecular forces get weaker, leading to decrease in viscosity as ϕ and *M* increase, therefore enhance the fluid temperature. The reverse happens with increasing *Ra*, therefore slow down the fluid temperature. Meanwhile, in figure 7, there exist weak intermolecular forces and decrease in viscosity which uniformly enhance the fluid temperature as angle of inclination and magnetic field parameter increase. With raising *Ra*, the intermolecular get stronger and viscosity increase leading to slow down in fluid temperature. Joule Heating effect is pertinent to the flow of electrically conducting fluid under the influence of magnetic field. The resistance Lorenz force on the flow due to the imposed magnetic field do lead to additional internal heat generation within the conducting fluid, consequently, the fluid temperature increases with increasing magnetic field intensity as shown in figures 6 and 7.

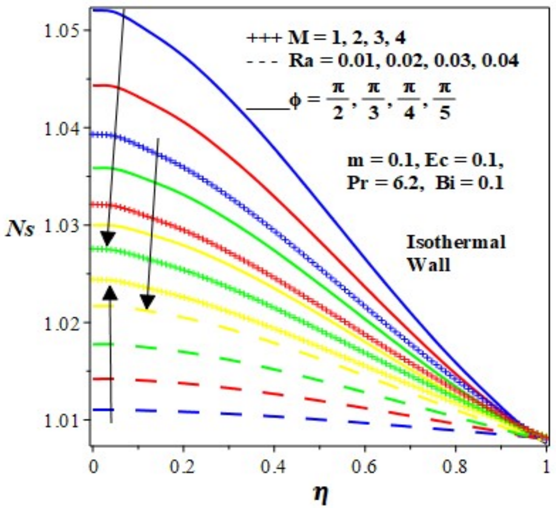

Fig. 10. Entropy profile with increasing ϕ , M and Ra

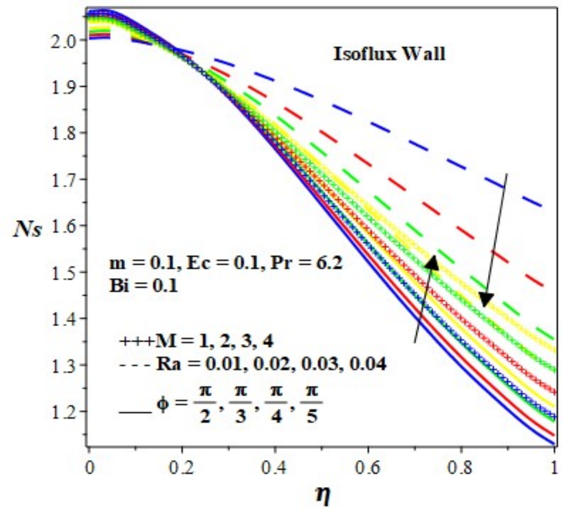

Fig. 11. Entropy profile with increasing ϕ , M and Ra

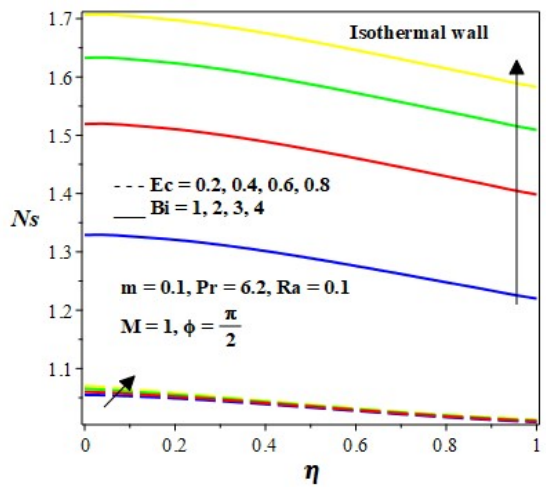

Fig. 12. Entropy profile with increasing Bi and Ec numbers

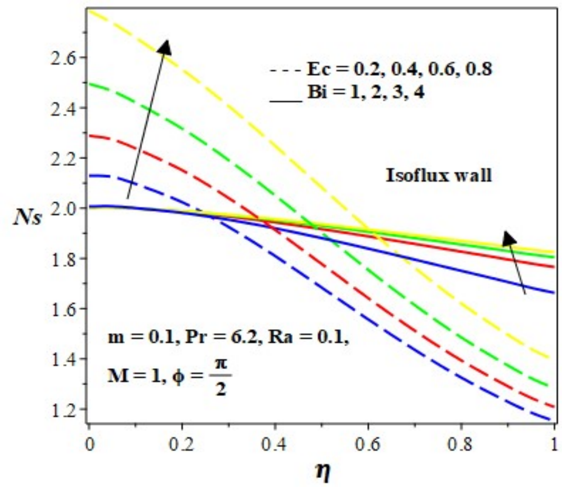

Fig. 13. Entropy profile with increasing Bi and Ec numbers

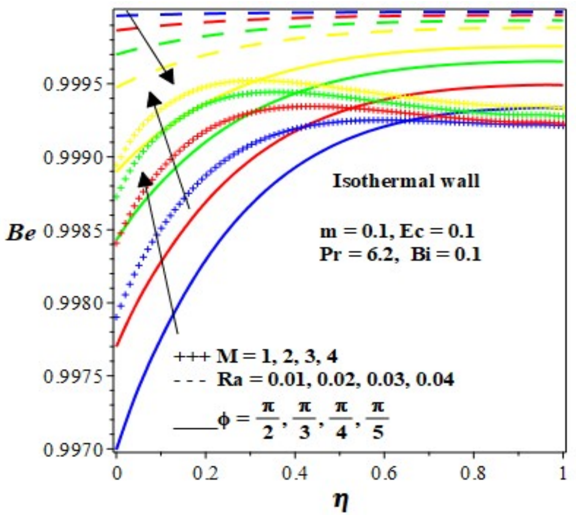

Fig. 14. The Bejan number profile with increasing ϕ , M and Ra

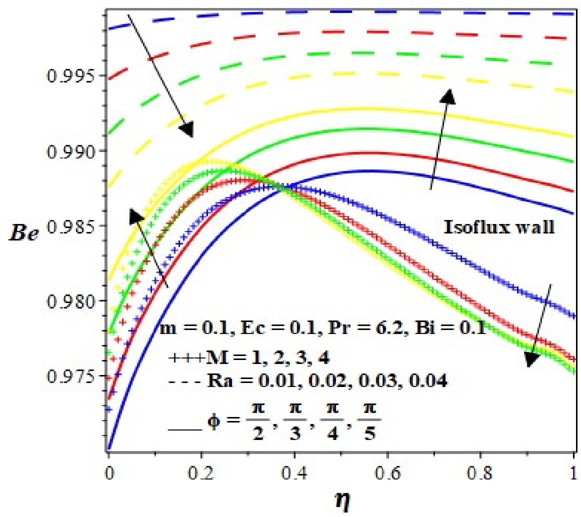

Fig. 15. The Bejan number profile with increasing ϕ , M and Ra

The same thing happens in figure 8 at free surface wall and figure 8 at both wall with increasing Biot number. Increase in *Ec* has no effect on fluid temperature as seen in figure 8 for isothermal wall but increases fluid velocity for isoflux as shown in figure 9. The effects of various changes in ϕ, Ra, M , Ec and Bi on entropy generation for both isothermal and isoflux are depicted in figures 10-13. It is noticed that the entropy generation decreases gradually at the wall surface and unites at the free surface for isothermal wall as the angle of inclination and magnetic field parameter gradually increase as shown in figure 10. This implies that increasing in values of ϕ and M slow down the entropy generation rate at the wall surface while increasing value of *Ra* accelerate entropy generation rate at wall surface. On the other hand, for the case of isoflux as illustrated in figure 11, it is noticed that the entropy generation slow down on the wall surface and increases on the free surface with increasing ϕ and *M*. It is noticed that entropy generation rate unites on wall surface but decreases on free surface with increasing *Ra*. The effects of *Ec* and *Bi* on both isothermal and isoflux wall are shown in figure 12 and 13. These figures show that entropy generation accelerates at both walls for isothermal with increasing Biot number and free surface for isoflux but has no effect on wall surface for isoflux. The increase in entropy generation rate in these figures show that the restrictive media exist caused high disorder in the fluid particle.

The effects of some parameters on the Bejan number are shown in figures 14-17. The graphs for isothermal shown that the Bejan number profile increases as parameters ϕ , *M* and *Bi* are increasing. This implies that irreversibility due to heat transfer dictate at the wall where increase in the Bejan number take place. For the same isothermal case in figure 14 and 16, the Bejan number decreases with increasing *Ra* and *Ec*, which implies that entropy generation due to viscous dissipation dominates. In figure 15, there exist cross flow as *M* is increasing. Th Bejan number rises at the wall surface and decreases at free surface. Figure 17 depicts the effect of *Ec* on the Bejan number. It is noticed that the Bejan number decreases as *Ec* is increasing. This therefore implies that, entropy generation due to viscous dissipation govern the flow processes at both surfaces.

Figures 18-19 show the effect of increasing the angle of inclination, magnetic field parameter versus Rayleigh number on skin friction. It is clearly seen from figures 18 and 19, as the angle of inclination versus Rayleigh number is increasing for both isothermal and isoflux wall, we realize that there is unity in the wall surfaces while decrease in the free surfaces were noticed. In these figures, as *M* is increasing for isothermal wall, the skin friction rise up and decline for isoflux but unite at the wall surfaces for both cases.

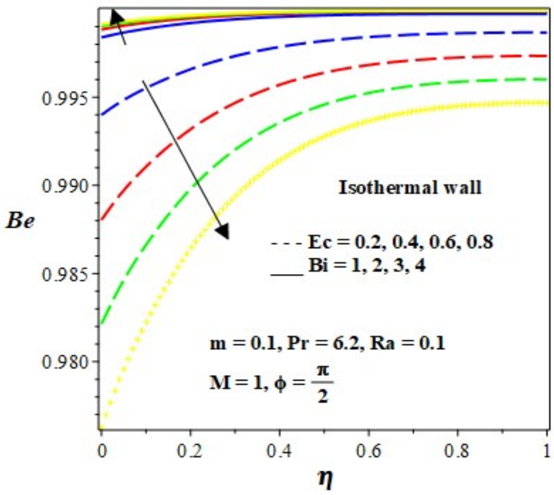

Fig. 16. The *Be* number profile with increasing *Bi* and *Ec* numbers

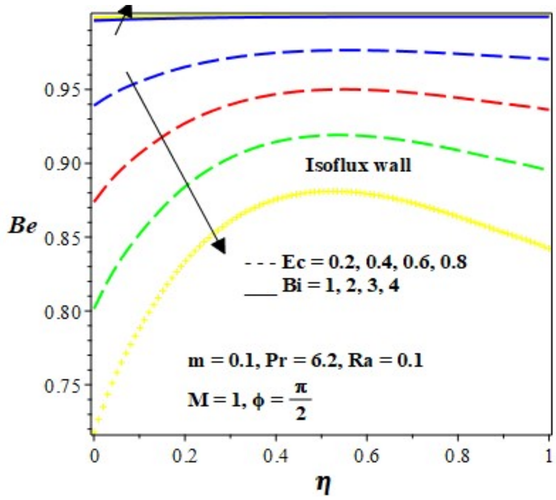

Fig. 17. The *Be* number profile with increasing *Bi* and *Ec* numbers

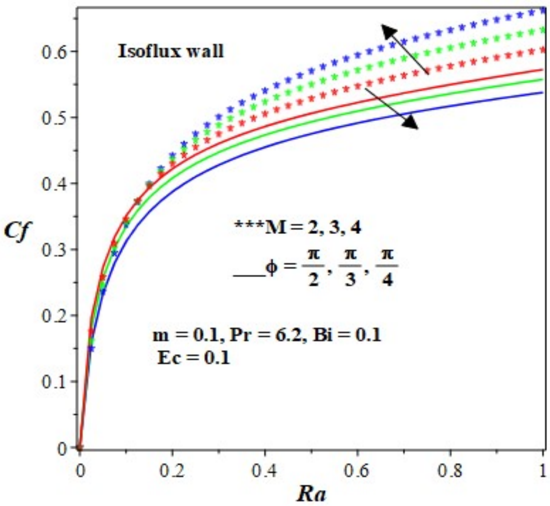

Fig. 18. Skin friction with increasing ϕ , *M* and *Ra*

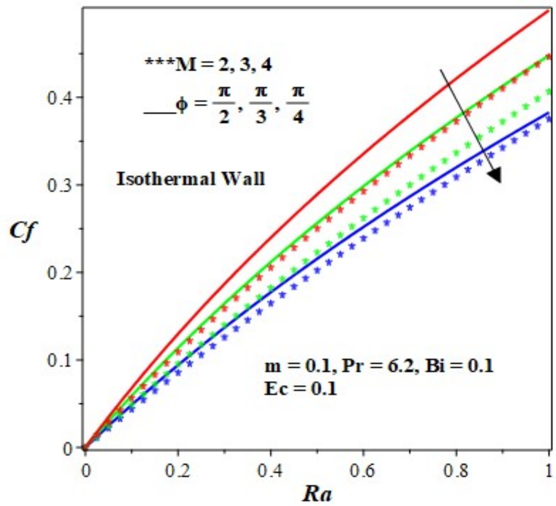

Fig. 19. Skin friction with increasing ϕ , *M* and *Ra*

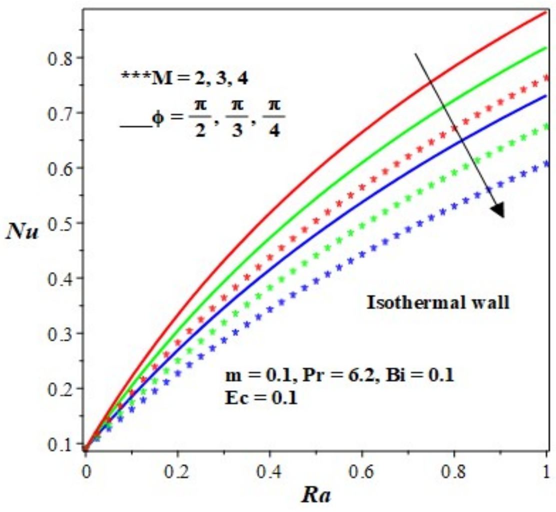

Fig. 20. *Nu* number with increasing ϕ , *M* and *Ra*

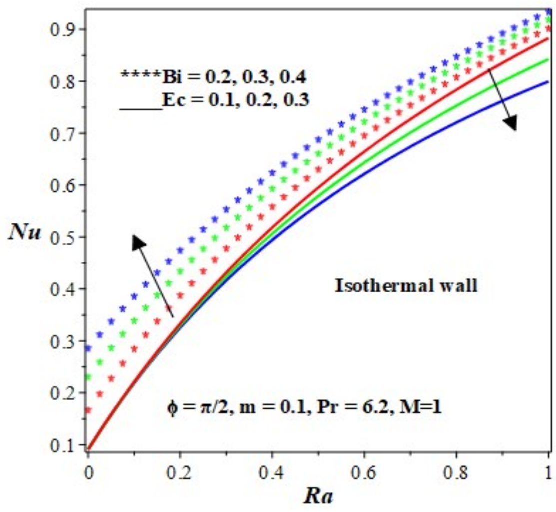

Fig. 21. *Nu* number with increasing *Ec*, *Bi* and *Ra*

The influences of magnetic field parameter, angle of inclination, Biot number and Eckert number versus Rayleigh number on isothermal wall are depicted in figures 20 and 21. It is noticed in figure 20 that increases in ϕ and *M* versus *Ra*, unite the Nusselt number at the wall surface but decreases the Nusselt number at the free surface. This implies that heat transfer at the wall surface by conductive and convective are relatively equal while at the free surface, heat transfer by conductive is more than convective thereby decrease the Nusselt number. In figure 21, the Nusselt number increase across the flow as *Bi* versus *Ra* are increasing.

4. Conclusion

Intrinsic irreversibility and heat transfer in a buoyancy-driven variable liquid film along both isothermal and isoflux walls inclined heated wall with convective cooling were explored. The fluid velocity and temperature contours were obtained. The mathematical expression for entropy generation rate, the Bejan number and skin friction were obtained. Our results concealed the following:

- Fluid velocity unites at heated wall surface and decreases at free surface with increasing ϕ , *M* and *Bi* increases at free surface with increasing *Ra* for both isothermal and isoflux walls
- Fluid temperature increases at the free surface with increasing ϕ , *M* and decrease with increasing *Ra*, *Bi* for isothermal wall. The fluid velocity increases at both surfaces with increasing ϕ , *M*, *Ec* and decrease with increasing *Ra*, *Bi* for isoflux wall
- For isothermal wall, entropy generation rate decreases at the heated wall surface with increasing ϕ , *M* and increases at the heated wall surface with increasing *Ra*, *Ec* but unite at free surface. For isoflux, increase in entropy generation rate is well pronounced at free surface with increasing ϕ , *M*, *Bi*, *Ec* and decrease while *Ra* increases.
- The Bejan number profiles increase with increasing ϕ , *M*, *Bi* and decrease with increasing *Ra*, *Ec* for both isothermal and isoflux cases
- The skin friction unites at wall surfaces for both isothermal and isoflux. It's decreases at free surface at isoflux with increasing ϕ , *M* versus *Ra* while it's increase with increasing *M* versus *Ra* and decrease with increasing ϕ versus *Ra*.
- Nusselt number for isothermal heated surface decreases at the free surface with increasing ϕ , *M*, *Ec* versus *Ra* while increasing with increase in *Bi* versus *Ra*.

Conflict of Interest

The author(s) declared no potential conflicts of interest with respect to the research, authorship and publication of this article.

Funding

The author(s) received no financial support for the research, authorship and publication of this article.

References

[1] Thiele, U., Knobloch, E., Thin liquid films on a slightly inclined heated plate. *Physica D*, 190 (2004) 213–248.

[2] Ern, A., Joubaud, R., Lelièvre, T., Numerical study of a thin liquid film flowing down an inclined wavy plane. *Physica D*, 240 (2011) 1714–1723.

[3] Ghiasy, D., Boodhoo, K.V.K., Tham, M.T., Thermographic analysis of thin liquid films on a rotating disc: Approach and challenges. *Applied Thermal Engineering*, 44 (2012) 39-49.
[4] Makinde, O.D., Hermite–Pade´ approximation approach to steady flow of a liquid film with adiabatic free surface along an inclined heat plate. *Physica A*, 381 (2007) 1–7.
[5] Sadiq, I.M.R., Usha, R., Linear instability in a thin viscoelastic liquid film on an inclined, non-uniformly heated wall. *International Journal of Engineering Science*, 43 (2005) 1435–1449.
[6] Makinde, O.D., Laminar falling liquid film with variable viscosity along an inclined heated plate. *Applied Mathematics and Computation*, 175 (2006) 80–88.
[7] Sekhar, G.N., Jayalatha, G., Elastic effects on Rayleigh-Benard convection in liquids with temperature-dependent viscosity. *International Journal of Thermal Sciences*, 49 (2010) 67–75.
[8] Nonino, C., Del Giudice, S., Savino, S., Temperature dependent viscosity effects on laminar forced convection in the entrance region of straight ducts. *International Journal of Heat and Mass Transfer*, 49 (2006) 4469–4481.
[9] Hooman, K., Gurgenci, H., Effects of temperature-dependent viscosity on Be´nard convection in a porous medium using a non-Darcy model. *International Journal of Heat and Mass Transfer*, 51 (2008) 1139–1149.
[10] Kabova, Y.O., Kuznetsov, V.V., Kabov, O.A., Temperature dependent viscosity and surface tension effects on deformations of non-isothermal falling liquid film. *International Journal of Heat and Mass Transfer*, 55 (2012) 1271–1278.
[11] Eegunjobi, A.S., Makinde, O.D., Entropy generation analysis in transient variable viscosity Couette ow between two concentric pipes. *Journal of Thermal Science and Technology*, 9(2), 2014, 8p.
[12] Vishnu Ganesha, N., Al-Mdallalb, Q.M., Chamkhac, A.J., A numerical investigation of Newtonian fluid flow with buoyancy, thermal slip of order two and entropy generation. *Case Studies in Thermal Engineering*, 13 (2019) 100376.
[13] Eegunjobi A.S., Makinde, O.D., MHD Mixed Convection Slip Flow of Radiating Casson Fluid with Entropy Generation in a Channel Filled with Porous Media. *Defect and Diffusion Forum*, 374 (2017) 47-66.
[14] Sourtiji, E., Gorji-Bandpy, M., Ganji, D.D., Seyyedi, S.M., Magnetohydrodynamic buoyancy-driven heat transfer in a cylindrical–triangular annulus filled by Cu–water nanofluid using CVFEM. *Journal of Molecular Liquids*, 196 (2014) 370-380.
[15] Parmar, L., Kulshreshtha, S.B., Singh, D.P., The role of magnetic field intensity in blood flow through overlapping stenosed artery: A Herschel-Bulkley fluid model. *Advances in Applied Science Research*, 4(6) (2013) 318-328.
[16] Astarita, G.M., Palumbo, G., Non-Newtonian gravity flow along inclined plane surfaces, *Industrial & Engineering Chemistry Fundamentals*, 3(4) (1964) 333-339.
[17] Makinde, O.D., Laminar falling liquid film with variable viscosity along an inclined heated plate, *Applied Mathematics and Computation*, 175 (2006) 80-88.
[18] Makinde, O.D., Thermodynamic second law analysis for a gravity-driven variable viscosity liquid film along an inclined heated plate with convective cooling. *Journal of Mechanical Science and Technology*, 24(4) (2010) 899-908.
[19] Saouli, S., Aiboud-Saouli, S., Second law analysis of laminar falling liquid film along an inclined heated plate. *International Communications in Heat and Mass Transfer*, 31 (2004) 879-886.
[20] Cebeci, T., Bradshaw. P., *Physical and Computational Aspects of Convective Heat Transfer*, Springer: New York, NY, USA, 1988.
[21] Afridi, M.I., Qasim, M., Khan, N.I., Makinde, O.D., Minimization of Entropy Generation in MHD Mixed Convection Flow with Energy Dissipation and Joule Heating: Utilization of Sparrow-Quack-Boerner Local Non-Similarity Method, *Defect and Diffusion Forum*, 387 (2018) 63-77.
[22] Khan, N.A., Naz, F., Sultan, F., Entropy generation analysis and effects of slip conditions on micropolar fluid flow due to a rotating disk, *Open Engineering*, 7 (2017) 185–198.